



HAL
open science

Particle-attached riverine bacteriome shifts in a pollutant-resistant and pathogenic community during a Mediterranean extreme storm event

Mégane Noyer, Brice Reoyo-Prats, Laurence Voutquenne-Nazabadioko, Maria Bernard, Olivier Verneau, Carmen Palacios

► To cite this version:

Mégane Noyer, Brice Reoyo-Prats, Laurence Voutquenne-Nazabadioko, Maria Bernard, Olivier Verneau, et al.. Particle-attached riverine bacteriome shifts in a pollutant-resistant and pathogenic community during a Mediterranean extreme storm event. *Science of the Total Environment*, 2020, 732, pp.139047. 10.1016/j.scitotenv.2020.139047 . hal-03162047

HAL Id: hal-03162047

<https://hal.science/hal-03162047>

Submitted on 3 Jun 2022

HAL is a multi-disciplinary open access archive for the deposit and dissemination of scientific research documents, whether they are published or not. The documents may come from teaching and research institutions in France or abroad, or from public or private research centers.

L'archive ouverte pluridisciplinaire **HAL**, est destinée au dépôt et à la diffusion de documents scientifiques de niveau recherche, publiés ou non, émanant des établissements d'enseignement et de recherche français ou étrangers, des laboratoires publics ou privés.



Distributed under a Creative Commons Attribution - NoDerivatives 4.0 International License

1 **Particle-attached riverine bacteriome shifts in a pollutant-resistant and pathogenic**
2 **community during a Mediterranean extreme storm event**

3

4 Mégane NOYER^{a,b}, Brice REOYO-PRATS^{a,b}, Dominique AUBERT^{a,b}, Maria BERNARD^{c,d},
5 Olivier VERNEAU^{a,b,e} & Carmen PALACIOS^{a,b,*}

6

7 ^a. Univ. Perpignan Via Domitia, CEFREM, UMR5110, F-66860, Perpignan, France

8 ^b. CNRS, CEFREM, UMR5110, F-66860, Perpignan, France

9 ^c. Univ. Paris-Saclay, INRAe, AgroParisTech, GABI, 78350, Jouy-en-Josas, France

10 ^d. INRAe, SIGENAE, 78350, Jouy-en-Josas, France

11 ^e. Unit. for Environmental Sciences and Management, North-West University, ZA-2520,
12 Potchefstroom, South Africa

13

14 * Corresponding author at: UPVD, CEFREM, UMR5110, F-66860 Perpignan, France.

15 E-mail address: carmen.palacios@univ-perp.fr (C. Palacios).

16 **Abstract**

17 Rivers are representative of the overall contamination found in their catchment area.
18 Contaminant concentrations in watercourses depend on numerous factors including land use
19 and rainfall events. Globally, in Mediterranean regions, rainstorms are at the origin of fluvial
20 multipollution phenomena as a result of Combined Sewer Overflows (CSOs) and floods.
21 Large loads of urban-associated microorganisms, including faecal bacteria, are released
22 from CSOs which place public health – as well as ecosystems – at risk. The impacts of
23 freshwater contamination on river ecosystems have not yet been adequately addressed, as
24 is the case for the release of pollutant mixtures linked to extreme weather events. In this
25 context, microbial communities provide critical ecosystem services as they are the only
26 biological compartment capable of degrading or transforming pollutants. Through the use of
27 16S rRNA gene metabarcoding of environmental DNA at different seasons and during a
28 flood event in a typical Mediterranean coastal river, we show that the impacts of
29 multipollution phenomena on structural shifts in the particle-attached riverine bacteriome
30 were greater than those of seasonality. Key players were identified via multivariate statistical
31 modelling combined with network module eigengene analysis. These included species highly
32 resistant to pollutants as well as pathogens. Their rapid response to contaminant mixtures
33 makes them ideal candidates as potential early biosignatures of multipollution stress. Multiple
34 resistance gene transfer is likely enhanced with drastic consequences for the environment
35 and human-health, particularly in a scenario of intensification of extreme hydrological events.

36

37 **Keywords**

38 microbial ecotoxicology; water quality; multipollution phenomena; coastal Mediterranean
39 rivers; sewer overflow; multiple stressors.

40 **1. Introduction**

41 Rivers are representative of the overall pollution in their catchment area (Giri and Qiu,
42 2016). Freshwaters near urban areas are particularly impacted by contaminants, from river
43 sediments derived from leakage and runoff as well as from in-sewer solids resuspension
44 when the sewerage system overflows during heavy rainfalls or during snow melting periods
45 (Madoux-Humery et al., 2013; Osorio et al., 2012; Oursel et al., 2014; Taghavi et al., 2011).
46 Globally, in Mediterranean climate regions, urban system overflows often occur because of
47 the recurrence of intense rainfalls (Cowling et al., 2005; Gasith and Resh, 1999; Reoyo-Prats
48 et al., 2017), while combined sewers, which simultaneously carry wastewater and
49 stormwater, are also common around the world (Commissariat Général au Développement
50 Durable, 2011; U.S. Environmental Protection Agency, 2016). When CSOs occur, large
51 loads of contaminant mixtures are discharged into surface waters not only from runoff but
52 from private residences as well (Llopart-Mascaró et al., 2014; Paillet et al., 2009; Phillips and
53 Chalmers, 2009; Reoyo-Prats et al., 2017; Weyrauch et al., 2010).

54 Mixtures of contaminants are recognised as a new major threat for freshwater
55 ecosystems (Sabater et al., 2019), but only heterotrophic microorganisms contribute to the
56 degradation or transformation of these organic or inorganic xenobiotics (Carles et al., 2019;
57 Díaz, 2004). As such, microbial communities provide critical ecosystem services.
58 Nevertheless, most environmental microbial ecotoxicology studies analyse a single
59 substance or contaminant family type, through a functional approach (Lambert et al., 2012;
60 Pesce et al., 2010a; Widenfalk et al., 2008) or through structural changes in microbial
61 communities together with contaminant concentrations (Amaral-Zettler et al., 2010; Lambert
62 et al., 2012; Palacios et al., 2008; Pesce et al., 2010b). Only few studies have examined the
63 *in situ* effect of pollutant mixtures with a focus on periphyton biofilms or sediment microbes
64 (Dorigo et al., 2010; Pesce et al., 2008). This highlights the need to assess shifts in the river
65 water bacteriome in response to multiple contaminants (Staley et al., 2014).

66 The impact of urban water discharges during storm and flood events on faecal
67 bacterial contamination (Baudart et al., 2000; Chu et al., 2011; Masters et al., 2016), nitrogen

68 or carbon cycles (Eyre and Ferguson, 2006; Fouilland et al., 2012), as well as on temporal
69 succession changes in microbial communities through microscopic enumeration (Fisher et
70 al., 1982; Muylaert and Vyverman, 2006), has been widely studied and has made clear the
71 negative impact of rainstorms on water quality and thus on human health (Ahern et al.,
72 2005). Recent studies have focused on tracking sources of urban-associated bacteria
73 released through sewer discharges or storm water (Besemer et al., 2005; Wu et al., 2010;
74 Newton et al., 2013; Fisher et al., 2015; Marti et al., 2017a, 2017b) but only two studies have
75 described bacterial community dynamics throughout the course of a rainstorm event (Kan,
76 2018; Ulrich et al., 2016). Although contaminant mixtures released during CSOs occur mainly
77 at first flushes compared to other moments of the event (Ashley et al., 1992; Reoyo-Prats et
78 al., 2017), bacterial community changes at first flushes have yet to be addressed.

79 In the transfer of chemical substances during storm events, suspended particles play
80 a fundamental role (Turner and Millward, 2002) as sediments and in-sewer solids act as both
81 sources and sinks for nutrients and contaminants (see above and also Amalfitano et al.,
82 2017). Particulate matter thus offers a broader niche differentiation to which microbes can
83 respond, resulting in a more diverse compartment of the fluvial microbiome (Savio et al.,
84 2015). Particle-associated bacteria, which refers to bacteria that form biofilms around
85 particles and large aggregates (Bartram and Ballance, 1996), are more reactive to changes
86 in water composition in both marine and limnetic environments (Besemer et al., 2005; Crump
87 et al., 1999; Savio et al., 2015). For these reasons and given the main purpose of our study,
88 rather than describing the whole microbial community, we concentrated on particle-attached
89 bacteria.

90 Our main objective was to finely assess shifts in the fluvial bacteriome evolution
91 along seasons and during a typical intense Mediterranean rainstorm event in comparison to
92 the dynamics of physicochemical parameters, including a large variety of contaminants. The
93 following questions were addressed: how is the diversity of the particle-attached bacterial
94 community impacted by the flood event when compared to seasonal diversity? Are structural
95 patterns of diversity driven by physicochemical dynamics along the extreme event? Do

96 contaminant mixtures impact the watercourse bacteriome differently at the beginning of a
97 storm in comparison to the flow peak? Are there specific ecotypes significantly related to
98 physicochemical dynamics?

99

100 **2. Material and Methods**

101 *2.1. Study site and sampling campaigns*

102 Campaigns took place at the Têt River, a typical Mediterranean coastal watercourse
103 with a torrential regime that discharges into the Gulf of Lion (Southeast of France) (Dumas et
104 al., 2015; Reoyo-Prats et al., 2017), at a site downstream from the Perpignan city wastewater
105 treatment plant, the main threat to the water quality of this river (Conseil Général des
106 Pyrénées Orientales (CG66), 2012, 2009; Reoyo-Prats et al., 2018, 2017). For a review on
107 the hydrology, biogeochemistry and anthropogenic impacts on the Têt River, as well as for
108 further details on sampling methodology, see Reoyo-Prats *et al.* (2017). Today, this river is
109 still predominantly impacted by agriculture and urbanisation void of any major industries or
110 farms within its catchment area. Samples were named according to sampling time (Fig. 1 for
111 details). Ten litres water samples for both chemicals and microbiology were collected during
112 periods of drought, in summer on the 17th September 2013 (SD sample) and in winter, on the
113 13th of February 2014 (WD sample). Then, in autumn, from 16th-21st November 2013, using
114 the same sampling protocol, we sampled a 5-year flood event 13 times over the course of
115 109 hours, with a high frequency sampling (1 h minimum intervals) at strategic moments:
116 before the event (t0 sample), at first flushes (t17-t19-t23), before the flow peak (t32-t37),
117 during the flow peak (t38-t41) and during the return to basal level water discharges (from t44
118 to t109).

119

120 *2.2. Field water samples processing and nucleic acids extraction*

121 Field samples were processed less than 2 hours after sampling. One litre mixed-
122 water sample from 10 L tank was entirely (or until clogged) filtered through 3 µm and 0.22
123 µm porosity cellulose acetate MF-Millipore membrane filters (Merck Darmstadt, Germany)

124 using a vacuum pump and a polysulfone filtration column (previously cleaned with HCl and
125 thoroughly rinsed with Milli-Q Water) placed in a bleach-cleaned bench of a laminar flow
126 hood. This operation was carried out three times to obtain three replicates per sample. Filters
127 were stored at -80 °C until nucleic acid extraction. Environmental nucleic acid extraction was
128 performed by resuspending filters in 425 µl lysis buffer (0.04 M EDTA, 0.05 M Tris, 0.75 M
129 sucrose). Filters were then subject to three 65°C liquid nitrogen cycles to mechanically break
130 cells. Lysozyme (Sigma-Aldrich, Merk) solution (1 mg/ml) was then added and placed in a
131 rotary mixer at 37°C (45 min). Next, Proteinase K (Sigma-Aldrich, Merk) was added (0.2
132 mg/ml) and filters were incubated at 55°C (1 h) with agitation every 10 minutes. AllPrep
133 DNA/RNA extraction kit (Qiagen, Hilden Germany) was finally used following manufacture
134 recommendations. DNA quantification was performed using a Nanodrop 2000 (Thermo
135 Fisher Scientific Wilmington, USA). A bacteria-targeted 16S rDNA PCR was performed to
136 verify DNA amplification of water samples and DNAs were stored at -80°C before sending
137 samples for sequencing.

138

139 *2.3. Metabarcoding of environmental DNA using the 16S rRNA gene and sequence* 140 *processing to form Operational Taxonomic Units (OTUs)*

141 DNA extractions were paired-end sequenced using Next Generation Sequencing
142 (NGS) Illumina MiSeq method (PE250). A pilot study with a single set of replicates from all
143 samples was first sent to Research and Testing Laboratories (RTL, Texas, USA). Two more
144 replicates were later sent to Genome Quebec laboratory (GQ, Montreal, Canada). Three
145 sample replicates already sequenced at RTL were also sent to GQ to be sequenced again.
146 These three double-sequenced replicates aimed to identify if differences in sequencing
147 methods between laboratories would yield different sequencing results in the same
148 replicates, which would impede a conjoint analysis. Sequencing targeted V3 and V4
149 hypervariable regions of the 16S rDNA by using 357wF (5'-CCTACGGGNGGCWGCAG-3')
150 and 785R (5'-GACTACHVGGGTATCTAATCC-3') universal bacterial primers (primer assay
151 list provided by RTL). To process sequences to form OTUs, we used FROGS (Find Rapidly

152 OTU pipeline v. r3.0-3.0, Escudié et al., 2018, see Supplementary A1). When relevant, multi-
153 affiliated OTUs were blasted using *blastn* on the NCBI nucleotide collection database
154 optimised for the highly similar sequences program.

155

156 2.4. Bacterial diversity analyses

157 Diversity analyses were performed using the output OTUs matrix, tree and
158 dissimilarity matrices calculated using FROGS as input for *Phyloseq* R package 1.24.2
159 (McMurdie and Holmes, 2013) and a collection of additional R functions
160 (<https://github.com/mahendra-mariadassou/phyloseq-extended>). Sequencing depth largely
161 influences alpha diversity, therefore we first checked reads number and rarefaction curves
162 for all replicates. While saturation was achieved in all of them, sequence depth was lower for
163 RTL sequenced replicates. Therefore, we analysed alpha diversity using non-filtered, non-
164 normalised replicates from GQ laboratory only. Alpha diversity was estimated using Fisher,
165 Simpson, Shannon and Pielou diversity indices and the non-parametric Chao1 species
166 richness estimator. The evolution of the diversity through time was statistically tested using
167 Kruskal-Wallis test (KW) followed by a post-hoc Dunn test on R software (v. 3.5.1, R Core
168 Team, 2018). Beta diversity was assessed after filtering out singletons/doubletons OTUs and
169 abundance normalisation to the sample with the lowest number of reads. Qualitative
170 (Jaccard and Unifrac) and quantitative (Bray-Curtis, Morisita and Weighted-Unifrac) indices
171 were first calculated with replicates separately. Outliers were neither observed for identical
172 replicates sent to both sequencing laboratories nor were they observed for all replicates of
173 the same sample, independent of sequencing laboratory origin. Thus, OTU abundances
174 were averaged over replicates. Sample dissimilarities were visualized using Principal
175 Coordinates Analysis (PCoA) and hierarchical clustering Ward.D2 method. A one-way
176 analysis of similarity (ANOSIM, Clarke, 1993) was performed to test for significant
177 differences between sample groups. The average abundances on filtered and normalised
178 counts were used for further analyses.

179

180 2.5. *Statistical analyses for inference*

181 2.5.1. *Constrained (canonical) ordination analyses*

182 Bacterial community diversity was assessed using the same samples as those used
183 to assess physicochemical environmental parameters in the 2013 storm event described
184 elsewhere (Reoyo-Prats et al., 2018, 2017). Analyses were processed with *vegan* R package
185 2.5-3 (Oksanen et al., 2018). To infer the relationship between environmental variables and
186 bacterial OTU abundances, we first checked collinearity through a statistical analysis of
187 environmental parameters only. The first step in constrained ordination was to resolve
188 collinear issues with environmental data. To do this, we performed a Principal Components
189 Multivariate Analysis (PCA) to explore the relationship among samples and physicochemical
190 parameters. We then performed Spearman correlations due to the non-normality and non-
191 homoscedasticity of the data. Finally, we tested for collinearity using variance inflation factor
192 (VIF) when performing constrained analyses. Variables with VIF > 10 were partialled out
193 (O'brien, 2007). The matrix of retained variables was standardised for further analyses.

194 Constrained ordination methods are robust multivariate analyses that facilitate both
195 pattern recognition in noisy data and statistical testing of the relationships between
196 organisms and the environment. Using detrended correspondence analysis, (DCA) the
197 gradient length of OTUs dataset was 3.58, so both canonical correspondence (CCA) and
198 redundancy analyses (RDA) were performed (ter Braak, 1987). For RDA, a Hellinger
199 transformation (Legendre and Gallagher, 2001) was performed. Also, a distance-based
200 redundancy analysis (dbRDA) was performed with dissimilarity indices from the previous
201 section. We then used permutation analyses of variance to evaluate significance of full
202 constrained models, constrained axis and terms. Variables were tested by adding each
203 variable independently. Triplots were then obtained with scaling focused on inter-species
204 distances. We further determined what OTUs best responded to environmental variables by
205 dividing the OTU matrix into $\geq 0.005\%$ and $< 0.005\%$ of total read number (1 017 326 reads)
206 following Bokulich *et al.* (2012) and repeating CCA/RDA modelling (DCA rendered a gradient
207 length of 3.42), to finally calculate, over most performant model, each OTU goodness of fit

208 (GOF). OTUs retained for further analyses had a $GOF \geq GOF_{average}$, which constitutes a
209 conservative approach to OTU selection.

210

211 *2.5.2. Network and module eigengene analyses*

212 In order to group OTUs with same abundance profiles, network analysis was
213 conducted on OTUs with $GOF \geq GOF_{average}$ (see 2.5.1 section), using the Molecular
214 Ecological Network Analyses Pipeline (MENAP: <http://ieg4.rccc.ou.edu/MENA/>, Deng et al.,
215 2012) with default parameters with two exceptions. First, zero counts were replaced by 0.01.
216 Second, as we used an already curated dataset according to environmental parameters,
217 OTUs present in at least one sample were retained to do not loose OTUs specific to one
218 sample. Random matrix theory (RMT)-based method was used to construct the network
219 using the automatically generated similarity threshold value (0.89). For network modularity
220 properties, greedy modularity optimization (Newman, 2006) rendered the highest modularity
221 value (0.46). To reveal a higher order of organisation among modules through an analysis of
222 their relationship with environmental parameters, a module eigengene analysis (Langfelder
223 and Horvath, 2007) was performed on MENAP using default parameters. This constrained
224 network was visualised in Cytoscape software (v. 3.7.1, Shannon et al., 2003).

225

226 **3. Results**

227 *3.1. Particle-attached bacterial diversity changes in the Têt River*

228 To study urban bacteriome dynamics, a high-resolution sampling of river water was
229 performed during a heavy rain event in autumn 2013. A pilot study demonstrated that
230 particle-attached bacteria were more diverse and heterogeneous than free-living bacteria
231 (Reoyo-Prats, 2014), which supported our decision to focus on this part of the community
232 only. Summer and winter drought periods were also sampled for comparison. A total of 392
233 443 operational taxonomic units (OTUs) corresponding to 1 084 527 reads were identified of
234 which 92% were singletons and 3% were doubletons. The vast majority of OTUs (99.8%)
235 was assigned to the bacterial domain. Chloroplasts, which represented 64 928 reads, were

236 removed. Alpha diversity statistical analyses showed significant differences among samples
237 for all indices (Table B1, $KW < 0.05$) except Fisher ($p = 0.068$, not shown). Fisher had the same
238 evolution pattern along time as the observed OTU number (Fig. B1a), which significantly
239 decreased just before the flow peak (t37) with respect to samples t17-t23. Estimated OTU
240 number (Chao1 index) significantly increased at the flow peak (Fig. B1b) and significantly
241 decreased only at the end of the flood. Shannon, Simpson and Pielou indices (Fig. B1c-e
242 respectively) revealed a significantly low diversity and evenness at t19 compared to t32.
243 While the Simpson index was significantly higher from t32 onward, Shannon and Pielou
244 indices decreased later at the flow peak and then increased significantly at t44. Alpha
245 diversity at drought periods did not show any major differences from t0.

246 For beta diversity, 9 211 OTUs (8 479 sequences/sample) were obtained after
247 filtering and normalisation. Jaccard and Unifrac qualitative dissimilarities differentiated two
248 communities, one included summer and winter drought samples (SD, WD) and a second
249 included samples collected at the beginning of the autumn storm event (t0-t37), from the rest
250 of the autumn samples (Fig. A1a-b). Flow peak samples (t38-t41), clustered together only
251 when phylogeny with Unifrac was considered. When OTU abundances were applied using
252 Morisita and Bray Curtis dissimilarities (Fig. A1c-d), autumn t0 sample clustered with summer
253 and winter droughts while the other relationships among samples remained largely
254 unchanged except that t38 clustered closer to post-flood samples with Morisita only. When
255 phylogenetic relationships using Weighted-Unifrac (Fig. 2a-b) were also considered: i) t0, as
256 well as summer and winter drought samples, clustered together; ii) t38 and t41 formed
257 another group; iii) t32 and t37 clustered with samples at the end of the flood (t44-t109); and
258 iv) t17 to t23 samples formed a new a more divergent group when compared with results
259 obtained with other dissimilarity measures. Analysis of similarity (ANOSIM) confirmed all four
260 (i to iv, above) community groups (Fig. 2) were significantly different among one another
261 ($p < 0.001$, $R = 0.78$). Phyla relative abundances and heatmap plot confirmed structuration in
262 four groups (Fig. 2c-d). Although the summer drought sample was slightly different from t0
263 and winter drought samples as a result of a larger amount of Actinobacteria, the first major

264 structural change occurred at t17 and lasted until t23, with a gain in Epsilonbacteraeota and
265 Firmicutes at the expense of Proteobacteria and, to a lesser extent, Bacteriodetes. These
266 last two phyla remained proportionally high at t32 and t37 to decrease only at the flow peak.
267 Proteobacteria abundance increased at these two intermediate samples, but really exploded
268 at t38 and t41, thus representing the second major temporal bacteriome change, reflected
269 also by the increase of Planctomycetes and the decrease of all other major phyla. Then, we
270 observed an inverse in the pattern, where Proteobacteria decreased and most other major
271 phyla increased.

272

273 3.2. *Linking the bacteriome to multiple contaminants dynamics through constrained* 274 *multivariate analyses*

275 During the same flood event of autumn 2013, Reoyo-Prats *et al.* (2018, 2017) studied
276 the dynamics of all known contaminant families. A statistical analysis of these parameters
277 (Supplementary A2 for details) allowed seven major environmental dynamics to be retained
278 (Fig. 1). To determine if different environmental dynamics could statistically explain observed
279 community shifts in diversity through time, we used several constrained multivariate
280 analyses. Significance and percentage of variance explained by all models tested are
281 summarised in Table 1a. Although all models were significant with the exception of CCA,
282 Morisita and Weighted-Unifrac dbRDA models performed best ($p < 0.001$). A strong
283 relationship between the two significant canonical axes and the environmental parameters
284 could be observed, with up to six dynamics being significant, Dyn1 to 3, 2,4-
285 Dichlorophenoxyacetic acid (2.4D), Diuron and NO_3^- (Table 1b, Fig. A3).

286

287 3.3. *Revealing OTUs significantly related to environmental parameters*

288 To further explore the relationship between the fluvial bacteriome and the
289 environmental parameters, we split the normalised abundance OTU matrix into OTUs \geq
290 0.005% of total abundance and those $< 0.005\%$. While no-significant models were obtained
291 with the second dataset, RDA and CCA models, which allow for the calculation of OTUs

292 goodness of fit (GOF), gained resolution with the $\geq 0.005\%$ dataset (602 OTUs) (Table A1).
293 The RDA model best explained our data (Fig. 3). A total of 260 OTUs best fitted to this model
294 ($GOF \geq 0.26$) and were submitted to network analysis in order to determine biological
295 interactions. The resulting network (R^2 of the power law=0.874) was composed of 17
296 modules with 167 nodes and 725 links (Fig. A4). Module membership and eigengene
297 correlations obtained from module eigengene analysis identified OTUs that were significantly
298 represented in each module (Table C1). Only the 13 modules that were significantly
299 correlated to environmental dynamics were retained for further analyses. Module 1 was
300 correlated to Dyn2, Dyn3 and Diuron and included 38 OTUs of which 13 were significant
301 (Fig. 4) comprising a total of 17 851 out of 24 625 reads from retained OTUs (72.5%, Table
302 C1). Most OTUs in this module were in samples t17, t19 and t23 and belonged to
303 Epsilonbacteraeota phylum. Bacteroidetes, Firmicutes and Patescibacteria phyla were also
304 abundant (Fig. C1a). OTU5, assigned to *Arcobacter cryaerophilus* (Epsilonbacteraeota), was
305 particularly abundant (75.3% of reads in Module 1 and 55.6% of retained OTU abundances,
306 Table C1). Three out of six Bacteroidetes OTUs were the most abundant, OTU41,
307 *Bacteroides graminisolvens*, OTU126, *Macellibacteroides fermentans* and OTU95,
308 *Cloacibacterium normanense*. Module 2 was related to Dyn 1. It included 33 OTUs from
309 which 24 were significant (Fig. 4) comprising a total of 3 585 reads (15% of retained OTU
310 abundances, Table C1). OTUs from this module were present in the summer drought
311 sample, at the beginning of the flood, and even more so at the flow peak (t38, Fig. C1b).
312 Proteobacteria was by far the most abundant phylum, particularly Rhodobacteraceae and
313 Sphingomonadaceae families within class Alphaproteobacteria. Two OTUs were highly
314 present from these families, respectively, OTU146 affiliated to *Trabizicola* sp. and OTU90
315 *Porphyrobacter donghaensis*, while OTU145, *Cloacibacillus* sp. was unique from the second
316 most abundant phylum, Synergistetes. Modules 3, 5, 7, 8, 9 and 11 comprised 6.4% of
317 retained OTU abundances (1 571 reads, Table C1) and were related to 2.4D dynamic (Fig.
318 4). OTUs in these modules peaked mainly at t41 (Fig. C1c). The most abundant were
319 OTU1184 belonging to Rickettsiales order and OTU790 belonging to Gemmataceae family,

320 with no clear phylogenetic affiliations. The rest of the modules, overall represented less than
321 7% of retained OTU abundances (Table C1, Fig. C1d-g).

322

323 **4. Discussion**

324 *4.1. Particle-attached riverine bacterial community shifts are driven by water* 325 *discharges and sewer overflows during Mediterranean rainstorms*

326 Studies that follow the ecological succession of microbial communities throughout
327 rainstorms are very scarce in the literature (Kan, 2018; Ulrich et al., 2016). Earlier studies
328 that described temporal changes throughout the duration of flood events using microscopic
329 enumeration found bacteria invariant along the succession (Fisher et al., 1982; Muylaert and
330 Vyverman, 2006). The impact of stormwater and floods on faecal bacteria loads are a major
331 sanitary concern and have earned sustained attention from researchers for decades (Ahern
332 et al., 2005). Comparatively, the non-faecal counterpart has received little attention, yet they
333 can be used as biosignatures to track sources of faecal pollution (Fisher et al., 2015; Newton
334 et al., 2013) perhaps to a better extent than the current faecal indicators used as sentinels of
335 human pathogens (McLellan et al., 2015; McLellan and Eren, 2014; Staley et al., 2014; Wu
336 et al., 2010). In this study, we sought to evaluate temporal succession in particle-attached
337 riverine bacteria using high-throughput sequencing of water samples from summer, winter
338 and autumn as well as during an autumn storm event that included a 5-year flood which led
339 to a peak instantaneous discharge of more than 250 m³/s. A thorough knowledge of the
340 coastal Mediterranean Têt River hydrodynamics (Dumas et al., 2015) allowed for fine-scale
341 sampling at crucial moments of the rainstorm and we observed that major changes in the
342 community diversity coincided with major changes in river flow. The base level autumn
343 community captured at t0 (where starting sampling time actually began before the storm
344 event), was more similar to bacterial assemblages associated with winter and summer
345 droughts than to those which emerged during the storm event ($p < 0.001$, Fig. 2). Throughout
346 the storm, a first major community shift occurred at first flushes (t17-t23, Fig. 2), coinciding
347 with CSOs (Reoyo-Prats et al., 2017). At this point in time we noticed the highest proportion

348 of Epsilonbacteraeota and Firmicutes, commonly detected in sewage and sewer biofilms
349 (McLellan and Roguet, 2019). During this phase, observed diversity and Fisher index were
350 the highest, while Shannon, Pielou and Simpson indices were significantly lower indicating a
351 community skewness (Fig. B1a-e). We hypothesize that CSOs brought new microorganisms
352 into waters derived not only from runoff and wastewater, but also from the washout of in-
353 sewer deposits, destabilizing the fluvial bacterial consortium (Fig. B1). This hypothesis is
354 reinforced by *Escherichia coli* counts, which were highest at this same moment (Fig. A2).
355 Ulrich *et al.* (2016) performed a microbial study on a Pennsylvania stream (USA) during a
356 100-year river flood of 200 m³/s, where *E. coli* abundance peaked at the highest flow level,
357 which according to authors originated from previous sewer overflows. In our study, *E. coli*
358 also peaked at the highest river discharge but counts were much lower than those during first
359 flushes (Reoyo-Prats *et al.*, 2017), which thus far, have not been studied in-depth. Ulrich *et*
360 *al.* (2016) concluded that hydrodynamic changes structured bacterial communities as a result
361 of differences in composition and diversity after the flow peak, with an increase of Firmicutes
362 observed in some flow peak samples. In our study, a second major community shift occurred
363 at the highest water discharge (t38-t41), where we observed an increase of Proteobacteria
364 and Planctomycetes. As in the Pennsylvania stream, we also noticed the highest presence of
365 Firmicutes before and after this specific moment (t37, t44-t61, Fig. 2c). In contrast, t38 and
366 t41 had the lowest observed and Shannon diversities but the highest Chao1 index (Fig. B1a-
367 b), in other words, the Chao1 considered that not all the diversity had been sampled although
368 saturation of rarefaction curves was reached. One hypothesis which may explain these
369 contradictory results between parametric and non-parametric diversity indices, is that high
370 quantities of attached-bacteria are washed-out from particles at the flow peak. This
371 hypothesis is supported by the low equitability of these samples (Fig. B1e) in spite of having
372 the lowest number of OTU counts among all samples (Fig. B1a). In the Pennsylvania storm
373 event, both the highest evenness, Chao1 and observed diversities were obtained at the flow
374 peak (Ulrich *et al.*, 2016). Similarly, Kan (2018), who studied two small floods, obtained
375 inversed patterns for Simpson and Shannon indices compared to ours. These results

376 reinforce our hypothesis because they studied the whole community and not only attached
377 bacteria. However, as we used replicates, statistical analyses were possible. Shannon,
378 Simpson and Pielou indices at the flow peak samples were not significantly different to most
379 of the other samples. After t38 and t41 samples, alpha diversity increased significantly,
380 demonstrating the contribution of a more diverse upstream bacteriome (Savio et al., 2015)
381 following runoff and rapid downflow. Finally, bacterial composition at the end of our sampling
382 time, 4.5 days after t0 i.e. sample t109, was similar to t32 and t37, pointing towards
383 community resilience (Fig. 2). Additionally, when summer and winter drought samples were
384 excluded and only autumn samples were analysed (not shown), t0 (the flow base level
385 community) grouped together with t32 and t37 samples, further supporting the evidence of
386 the evolution towards a recovery of the fluvial community after the rainstorm. Apart from
387 Ulrich *et al.* (2016), who also noticed community resilience five days after the storm, fluvial
388 bacteriome recovery upon perturbation is hardly addressed in the literature and needs further
389 attention.

390

391 4.2. *Tracking microbial structural community changes according to environmental* 392 *parameters: what is new?*

393 Along with the study of riverine bacteriome shifts during a typical Mediterranean
394 heavy rain event, we analysed a large selection of physicochemical parameters including
395 pollutants such as pesticides, trace metals or pharmaceuticals. Studies with such a detailed
396 follow-up are rare (Staley et al., 2014). Thanks to advances in NGS methods, research in
397 environmental microbiology has entered into a new era where the driving forces exerted by
398 environmental parameters can now be deeper explored than never envisaged before.
399 Although the explanatory power of constrained multivariate gradient analysis for inference on
400 how environmental parameters shape microbial community structures had already been
401 demonstrated (Besemer et al., 2005; Ghiglione et al., 2008), how riverine communities are
402 finely shaped by chemical inputs remained poorly studied prior to the NGS era, with few
403 exceptions in extreme habitats with low diversity (Amaral-Zettler et al., 2010; Palacios et al.,

404 2008). As predicted by Ramette (2007), the power of high-throughput sequencing to capture
405 most diversity opened new possibilities for inference (Newton et al., 2013; Savio et al., 2015;
406 Staley et al., 2014). Most studies suggested that only very few taxa were influenced by
407 physicochemical parameters, while biotic interactions were the primary drivers of variation in
408 bacteriome structure, at least at a local scale (Fortunato and Crump, 2011; Staley et al.,
409 2014). In a comprehensive literature review of the influence of environmental factors on
410 stream microbiota, Zeglin (2015) raised the importance of pollutants such as metals
411 compared to nutrient load in altering these communities. Our results demonstrate that six
412 abiotic environmental dynamics linked to multicontamination phenomena derived from CSOs
413 and runoff (Fig. 1) acted as environmental driving forces of the particle-attached bacteriome
414 during a storm event (Fig. A4). Constrained analyses models based on beta diversity
415 dissimilarities matrix (dbRDA) were used to achieve these results (Table 1). Instead, models
416 CCA and RDA based on OTU abundance matrix were effective only when background noise
417 was reduced keeping OTUs $\geq 0.005\%$ of total reads (Fig. 3 and next section). Using
418 qualitative Jaccard dissimilarity index, 2.4D and Diuron dynamics significantly shaped
419 bacterial presence/absence differences among samples, but dynamics Dyn2 and Dyn3
420 became significant only when considering phylogeny with Unifrac dissimilarity (Table 1).
421 Quantitative Bray-Curtis, Morisita and Weighted-Unifrac indices also consider OTU
422 abundances, revealing which parameters affect bacterial growth. Globally, all parameters
423 except Dyn4, became significant in structuring samples. Surprisingly, Morisita rendered
424 similar results to Weighted-Unifrac, both captured nearly the same variance of the diversity
425 matrix (Table 1, 77% vs 73%). Thus, when phylogeny is not available, the Morisita
426 dissimilarity index is a very interesting alternative (Palacios et al., 2008).

427

428 4.3. *Key players involved in the response of particle-attached riverine bacteria to* 429 *environmental perturbations*

430 One of the greatest difficulties in the analysis of large high-throughput sequencing
431 datasets resides in deciding how to extract, analyse and synthesise the data to identify taxa

432 which play a key role in the studied processes. Here, we sought to identify ecotypes that
433 could act as key players in the riverine bacteriome response to rainstorm events. As such,
434 we first used an aggregation distance of 1 for clustering sequences into OTUs instead of the
435 classic 97% similarity. This method had a double purpose: 1) overcome the difficulty of using
436 a similarity cut-off criterion for defining significant units in microbial ecology (Cohan, 2006);
437 and 2) use an appropriate intraspecific level to find ecologically significant units (Acinas et
438 al., 2004; Palacios et al., 2008). We then reduced the dataset to OTUs $\geq 0.005\%$ of total
439 reads following Bokulich *et al.* (2012) and reconducted statistical analyses to retain OTUs
440 best adjusted to the most significant multivariate model. We finally used network analysis to
441 determine OTU associations according to their abundance profiles, that we then constrained
442 by module eigengene analysis (Deng et al., 2016; Zhou et al., 2011) to reveal key OTU
443 players driven by major environmental processes. This analysis allows for the calculation of
444 the significant correlation between module consensus abundance profile and environmental
445 constraints. Thus, it enabled us to go a step further, invoking identical driving forces which
446 underpin OTUs with strong memberships to the same module. This has been widely
447 assumed in functional genomics network analyses (Wolfe et al., 2005; Zhou et al., 2011).

448 According to our findings, shifts in particle-attached bacterial communities during
449 typical rainstorms in coastal Mediterranean rivers are driven by: 1) runoff and in-sewer solids
450 resuspension from CSOs at first flushes, and 2) runoff and riverbed sediment resuspension
451 at the flow peak (Fig. 5). The most notable key player driven by CSOs was *Arcobacter*
452 *cryaerophilus*, with significant membership to Module 1. *Arcobacter* genus is known to
453 represent a sewer signature (McLellan and Roguet, 2019; Newton et al., 2013) and *A.*
454 *cryaerophilus* is a human pathogen (Collado et al., 2010) with 25 antibiotic resistance
455 categories (Millar and Raghavan, 2017) and high potential capacity for horizontal gene
456 transfer to distant phylogenetic organisms (Jacquiod et al., 2017). Furthermore, Modules 1
457 and 4, correlated to Diuron, and/or Dyn2-3 released during CSOs (Fig. 5), contained several
458 Bacteroidetes which is commonly used as faecal indicator due to its high abundance in
459 warm-blooded animal faeces (Dick and Field, 2004). *Bacteroides graminisolvens*,

460 *Cloacibacterium normanense* and *Macellibacteroides fermentans* were particularly abundant.
461 These are relatively resistant species that are capable of surviving in extreme environments.
462 *C. normanense* removes heavy metals via production of extracellular polymeric substances
463 (Nouha et al., 2016) and *M. fermentans* degrades isosaccharinic acids linked to radioactive
464 wastes (Rout et al., 2017). Other key players during CSOs belonged to Firmicutes and
465 Fusobacteria, including OTUs from Ruminococcaceae a faecal-associated bacterial family
466 (McLellan et al., 2010; Newton et al., 2013) and Leptotrichiaceae, an underexplored family
467 common in gastrointestinal or urogenital tracts and oral cavities of humans and animals
468 (Eisenberg et al., 2016) (Fig. 5). The most remarkable finding from Module 2 was the
469 majority of Sphingomonadaceae and Rhodobacteraceae, which peaked at the flow peak,
470 suggesting these Alphaproteobacteria originated from terrestrial environments (Fig. 5).
471 Synergistaceae family was particularly abundant at the flow peak and during CSOs only,
472 concordant with Synergistetes frequent detection in wastewater (Jumas-Bilak and
473 Marchandin, 2014). In Modules linked to 2.4D, Gemmataceae, which are known for their
474 radiotolerance and complex cellular architectures (Mahajan, 2019), were highly abundant.
475 For instance, *Gemmata massiliana* (identity 87%) is a species isolated from hospital water
476 and resistant to beta-lactam antibiotics (Aghnatiou et al., 2015). Rickettsiales, also a major
477 order in these modules, is known to include mammalian pathogens such as *Orientia*
478 *tsutsugamushi* (identity 91%) causing scrub typhus (Darby et al., 2007). Finally, we also
479 found genera *Novosphingobium* and *Flavobacterium*, which are known to degrade 2.4D (Dai
480 et al., 2015; Silva et al., 2007). *Flavobacterium* sp. is also linked to the degradation of
481 organophosphate compounds such as pesticides (glyphosate, AMPA...) (Singh and Walker,
482 2006) (Fig. 5). In summary, key bacterial players from suspended solids emerging at crucial
483 moments of the rainstorm event consisted of highly pathogenic and/or resistant to pollutants
484 taxa. Marti et al. (2017a) also noted in sediments accumulated in a detention basin, a
485 bacteriome evolution towards a specific community better adapted to a disturbed
486 environment. In a scenario such as the one described in the present study (Fig. 5), where
487 multipollution phenomena associated with CSOs and floods disturb resident particle-

488 associated communities, cross-resistance and co-resistance – leading to multiple resistance
489 bacteria – (SCENIHR, 2009), are enhanced because horizontal gene transfer is i) induced by
490 stressors such as antibiotics, metals or biocides (Bengtsson-Palme et al., 2018), and ii)
491 preferentially facilitated in particle-attached bacteria (Stewart, 2013; Amalfitano et al., 2017).
492 Our results therefore reveal that CSOs and floods pose a non-negligible threat to the
493 capacity of resident fluvial communities to prevent the spread of resistances (Jørgensen et
494 al., 2018), with significant consequences to both ecosystems and public-health. Further
495 research on community changes in association with extreme events will help to confirm key
496 players identified in this study as indicators of multipollution, a major challenge in combined
497 stressors research (Sabater et al., 2019).

498

499 **5. Conclusions**

500 This study is the first to identify a significant relationship between the *in situ* fluvial
501 bacteriome, river hydrodynamics and the major changes of physicochemical parameters,
502 including several families of contaminants (faecal indicators, trace metals, pesticides and
503 pharmaceuticals) and nutrients during a typical Mediterranean storm event. The combination
504 of tools used in this work was crucial to the success of the results: a finely designed
505 fieldwork, a focus on the particle-attached bacteriome compartment through 16S rRNA gene
506 metabarcoding sequencing, together with an inference analysis using constrained
507 multivariate and network module eigengene statistical tools. The riverine bacteriome reacted
508 stronger to changes in pollutant dynamics during the storm event than to environmental
509 changes according to seasons. We highlight major community shifts linked to multipollution
510 phenomena at two critical moments of the storm event: the flow peak and the CSOs.
511 Particle-attached resident bacterial communities became more specialised towards pollutant-
512 resistant bacteria, some of which were pathogenic and/or capable of transforming chemical
513 molecules. Our results clearly illustrate how urban wastewater management practices can
514 trigger shifts from resident riverine communities to perturbed microbial assemblages, a
515 situation which is of particular concern with respect to human-health. Even though resilience

516 was achieved, ecosystems and human-health are likely at risk because co-resistance and
517 cross-resistance are typically enhanced in a scenario of continuous disturbance of resident
518 bacterial communities subjected to multipollution phenomena from CSOs and floods.
519 Furthermore, given the current trend towards the intensification of extreme hydrological
520 events as a consequence of climate change and the increase in anthropogenic impacts such
521 as urbanisation, deforestation and agriculture, not only in Mediterranean regions but also
522 elsewhere in the world, the conclusions drawn from our study are of the utmost importance
523 for urban management practises. For instance, as CSOs happen frequently in coastal rivers
524 of Mediterranean regions around the world due to their particular torrential regimes under this
525 climate, our study's findings highlight the need to transition from combined towards separate
526 sewers as a priority for conservation action at least in these regions. The rapid and
527 significant response of riverine particle-attached bacteria to environmental perturbations
528 enhance the potential use of these microorganisms for rapid assessment of environmental
529 risk in aquatic ecosystems.

530

531 **Acknowledgements**

532 We are thankful to A. Sanchez-Garcia, J. Sola, N. Delsaut, S. Kunesch and C. Menniti
533 (CEFREM laboratory) for helping us during sampling. We are thankful to captain and crew
534 from the *Néreis* (Observatoire Océanologique de Banyuls, France). We want to thank J.-F.
535 Ghiglione (LOMIC) for a first version of nucleic acids extraction protocol. We thank Research
536 and Testing Laboratories for kindly providing NGS primer assay list. We would like to
537 acknowledge Carles Ubeda Morant group (FISABIO, Valencia, Spain) for providing initial
538 help on data analyses and the Genotoul bioinformatics platform *Toulouse Midi-Pyrénées* and
539 *Sigenae* group (Toulouse, France) for providing help along the 16S rRNA gene
540 metabarcoding sequencing analysis and for providing computing and storage resources
541 (<http://bioinfo.genotoul.fr/>). We also thank to D. Ning and N. Xiao for MENAP support
542 (<http://ieg4.rccc.ou.edu/mena/main.cgi>). We also thank two anonymous reviewers for their

543 inputs and criticisms to an earlier version of the manuscript and to Jeanine Almany for his
544 professionalism when helping us editing the manuscript.

545

546 **Funding**

547 This work was supported by scholarships from *Ecole Doctorale Energie et Environnement*
548 (E2-UPVD) to BRP (n. 2014-ED.305-05) and to MN (n. 2017-19-ED.305) and from *Region*
549 *Occitanie* to MN. Supporting projects were: DEBiMicro (2013 BQR CEFREM to CP),
550 StepBiodiv (2015-2017 VEOLIA-Eau Perpignan to OV); and DEBi2Micro (2016-17 EC2CO
551 CNRS INSU to CP).

552

553 **Declaration of interest**

554 All authors declare that they have no conflict of interest.

555

556 **Data availability**

557 Sequencing data are deposited on NCBI under BioProject ID PRJNA602803.

558 **Supporting Information**

559 Additional Supporting Information may be found in the online version of this article at the
560 publisher's web-site.

561

562 ***Appendix_A***

563 **Supplementary A1** Processing of sequence data to form OTUs.

564 **Supplementary A2** Results for statistical analyses of physicochemical environmental
565 variables.

566 **Fig. A1** Beta diversity based on additional dissimilarities.

567 **Fig. A2** Principal Component Analysis biplot of environmental parameters and samples.

568 **Fig. A3** Weighted Unifrac distance-based RDA triplot.

569 **Fig. A4** Resulting network from best-fitted OTUs to the RDA canonical model.

570 **Table A1** Summary of constrained multivariate statistical analyses based on OTUs \geq
571 0.005%.

572 **Table A2** Probability values from Spearman correlation test on environmental parameters.

573

574 ***Appendix_B***

575 **Table B1** Alpha diversity indices at the Têt River and general Kruskal-Wallis test results.

576 **Fig. B1a-e** Evolution of alpha diversity indices along time.

577

578 ***Appendix_C***

579 **Table C1** Significant key player OTUs.

580 **Fig. C1a-g** Taxonomy evolution along time in significant modules.

581 **References**

- 582 Acinas, S.G., Klepac-Ceraj, V., Hunt, D.E., Pharino, C., Ceraj, I., Distel, D.L., Polz, M.F.,
583 2004. Fine-scale phylogenetic architecture of a complex bacterial community. *Nature*
584 430, 551–554. <https://doi.org/10.1038/nature02649>
- 585 Aghnatiou, R., Cayrou, C., Garibal, M., Robert, C., Azza, S., Raoult, D., Drancourt, M., 2015.
586 Draft genome of *Gemmata massiliana* sp. nov, a water-borne Planctomycetes
587 species exhibiting two variants. *Standards in Genomic Sciences* 10, 120.
588 <https://doi.org/10.1186/s40793-015-0103-0>
- 589 Ahern, M., Kovats, R.S., Wilkinson, P., Few, R., Matthies, F., 2005. Global health impacts of
590 floods: Epidemiologic evidence. *Epidemiologic Reviews* 27, 36–46.
591 <https://doi.org/10.1093/epirev/mxi004>
- 592 Amalfitano, S., Corno, G., Eckert, E., Fazi, S., Ninio, S., Callieri, C., Grossart, H.-P., Eckert,
593 W., 2017. Tracing particulate matter and associated microorganisms in freshwaters.
594 *Hydrobiologia* 800, 145–154. <https://doi.org/10.1007/s10750-017-3260-x>
- 595 Amaral-Zettler, L.A., Zettler, E.R., Theroux, S.M., Palacios, C., Aguilera, A., Amils, R., 2010.
596 Microbial community structure across the tree of life in the extreme Río Tinto. *The*
597 *ISME Journal* 5, 42–50. <https://doi.org/10.1038/ismej.2010.101>
- 598 Ashley, R.M., Wotherspoon, D.J.J., Coghlan, B.P., McGregor, I., 1992. The Erosion and
599 Movement of Sediments and Associated Pollutants in Combined Sewers. *Water*
600 *Science and Technology* 25, 101–114. <https://doi.org/10.2166/wst.1992.0184>
- 601 Bartram, J., Ballance, R., 1996. *Water quality monitoring: a practical guide to the design and*
602 *implementation of freshwater quality studies and monitoring programmes*, 1st ed. ed.
603 E & FN Spon, London; New York.
- 604 Baudart, J., Grabulos, J., Barousseau, J.-P., Lebaron, P., 2000. *Salmonella* spp. and Fecal
605 Coliform Loads in Coastal Waters from a Point vs. Nonpoint Source of Pollution.
606 *Journal of Environment Quality* 29, 241.
607 <https://doi.org/10.2134/jeq2000.00472425002900010031x>

608 Bengtsson-Palme, J., Kristiansson, E., Larsson, D.G.J., 2018. Environmental factors
609 influencing the development and spread of antibiotic resistance. *FEMS Microbiology*
610 *Reviews* 42. <https://doi.org/10.1093/femsre/fux053>

611 Besemer, K., Moeseneder, M.M., Arrieta, J.M., Herndl, G.J., Peduzzi, P., 2005. Complexity
612 of Bacterial Communities in a River-Floodplain System (Danube, Austria). *Applied*
613 *and Environmental Microbiology* 71, 609–620. [https://doi.org/10.1128/AEM.71.2.609-](https://doi.org/10.1128/AEM.71.2.609-620.2005)
614 [620.2005](https://doi.org/10.1128/AEM.71.2.609-620.2005)

615 Bokulich, N.A., Subramanian, S., Faith, J.J., Gevers, D., Gordon, J.I., Knight, R., Mills, D.A.,
616 Caporaso, J.G., 2012. Quality-filtering vastly improves diversity estimates from
617 Illumina amplicon sequencing. *Nature Methods* 10, 57–59.
618 <https://doi.org/10.1038/nmeth.2276>

619 Carles, L., Gardon, H., Joseph, L., Sanchís, J., Farré, M., Artigas, J., 2019. Meta-analysis of
620 glyphosate contamination in surface waters and dissipation by biofilms. *Environment*
621 *International* 124, 284–293. <https://doi.org/10.1016/j.envint.2018.12.064>

622 Chu, Y., Salles, C., Tournoud, M.-G., Got, P., Troussellier, M., Rodier, C., Caro, A., 2011.
623 Faecal bacterial loads during flood events in Northwestern Mediterranean coastal
624 rivers. *Journal of Hydrology* 405, 501–511.
625 <https://doi.org/10.1016/j.jhydrol.2011.05.047>

626 Clarke, K.R., 1993. Non-parametric multivariate analyses of changes in community structure.
627 *Austral Ecology* 18, 117–143. <https://doi.org/10.1111/j.1442-9993.1993.tb00438.x>

628 Cohan, F.M., 2006. Towards a conceptual and operational union of bacterial systematics,
629 ecology, and evolution. *Philosophical Transactions of the Royal Society B: Biological*
630 *Sciences* 361, 1985–1996. <https://doi.org/10.1098/rstb.2006.1918>

631 Collado, L., Kasimir, G., Perez, U., Bosch, A., Pinto, R., Saucedo, G., Huguet, J.M.,
632 Figueras, M.J., 2010. Occurrence and diversity of *Arcobacter* spp. along the
633 Llobregat River catchment, at sewage effluents and in a drinking water treatment
634 plant. *Water Research* 44, 3696–3702. <https://doi.org/10.1016/j.watres.2010.04.002>

635 Commissariat Général au Développement Durable, 2011. Le service d'assainissement en
636 France : principales données 2008. (No. 210).

637 Conseil Général des Pyrénées Orientales (CG66). Suivi de la qualité des cours d'eau du
638 bassin versant de la Têt Année - Rapport final année 2009., n.d.

639 Conseil Général des Pyrénées Orientales (CG66). Suivi de la qualité des cours d'eau du
640 bassin versant de la Têt Année - Rapport final année 2012., n.d.

641 Cowling, R.M., Ojeda, F., Lamont, B.B., Rundel, P.W., Lechmere-Oertel, R., 2005. Rainfall
642 reliability, a neglected factor in explaining convergence and divergence of plant traits
643 in fire-prone mediterranean-climate ecosystems. *Global Ecology and Biogeography*
644 14, 509–519. <https://doi.org/10.1111/j.1466-822X.2005.00166.x>

645 Crump, B.C., Armbrust, E.V., Baross, J.A., 1999. Phylogenetic Analysis of Particle-Attached
646 and Free-Living Bacterial Communities in the Columbia River, Its Estuary, and the
647 Adjacent Coastal Ocean. *Applied and Environmental Microbiology* 65, 3192.

648 Dai, Y., Li, N., Zhao, Q., Xie, S., 2015. Bioremediation using *Novosphingobium* strain DY4 for
649 2,4-dichlorophenoxyacetic acid-contaminated soil and impact on microbial community
650 structure. *Biodegradation* 26, 161–170. <https://doi.org/10.1007/s10532-015-9724-7>

651 Darby, A.C., Cho, N.-H., Fuxelius, H.-H., Westberg, J., Andersson, S.G.E., 2007. Intracellular
652 pathogens go extreme: genome evolution in the Rickettsiales. *Trends in Genetics* 23,
653 511–520. <https://doi.org/10.1016/j.tig.2007.08.002>

654 Deng, Y., Jiang, Y.-H., Yang, Y., He, Z., Luo, F., Zhou, J., 2012. Molecular ecological
655 network analyses. *BMC Bioinformatics* 13, 113. <https://doi.org/10.1186/1471-2105-13-113>

656

657 Deng, Y., Zhang, P., Qin, Y., Tu, Q., Yang, Y., He, Z., Schadt, C.W., Zhou, J., 2016. Network
658 succession reveals the importance of competition in response to emulsified vegetable
659 oil amendment for uranium bioremediation: Competition in bioremediation system.
660 *Environmental Microbiology* 18, 205–218. <https://doi.org/10.1111/1462-2920.12981>

661 Díaz, E., 2004. Bacterial degradation of aromatic pollutants: A paradigm of metabolic
662 versatility. *International Microbiology* 7, 173–180. <https://doi.org/im2304027> [pii]

663 Dick, L.K., Field, K.G., 2004. Rapid Estimation of Numbers of Fecal Bacteroidetes by Use of
664 a Quantitative PCR Assay for 16S rRNA Genes. *Applied and Environmental*
665 *Microbiology* 70, 5695–5697. <https://doi.org/10.1128/AEM.70.9.5695-5697.2004>

666 Dorigo, U., Berard, A., Rimet, F., Bouchez, A., Montuelle, B., 2010. In situ assessment of
667 periphyton recovery in a river contaminated by pesticides. *Aquatic Toxicology* 98,
668 396–406. <https://doi.org/10.1016/j.aquatox.2010.03.011>

669 Dumas, C., Ludwig, W., Aubert, D., Eyrolle, F., Raimbault, P., Gueneugues, A., Sotin, C.,
670 2015. Riverine transfer of anthropogenic and natural trace metals to the Gulf of Lions
671 (NW Mediterranean Sea). *Applied Geochemistry* 58, 14–25.
672 <https://doi.org/10.1016/j.apgeochem.2015.02.017>

673 Eisenberg, T., Fawzy, A., Nicklas, W., Semmler, T., Ewers, C., 2016. Phylogenetic and
674 comparative genomics of the family Leptotrichiaceae and introduction of a novel
675 fingerprinting MLVA for *Streptobacillus moniliformis*. *BMC Genomics* 17(1), 864.
676 <https://doi.org/10.1186/s12864-016-3206-0>

677 Escudié, F., Auer, L., Bernard, M., Mariadassou, M., Cauquil, L., Vidal, K., Maman, S.,
678 Hernandez-Raquet, G., Combes, S., Pascal, G., 2018. FROGS: Find, Rapidly, OTUs
679 with Galaxy Solution. *Bioinformatics* 34, 1287–1294.
680 <https://doi.org/10.1093/bioinformatics/btx791>

681 Eyre, B.D., Ferguson, A.J.P., 2006. Impact of a flood event on benthic and pelagic coupling
682 in a sub-tropical east Australian estuary (Brunswick). *Estuarine, Coastal and Shelf*
683 *Science* 66, 111–122. <https://doi.org/10.1016/j.ecss.2005.08.008>

684 Fisher, J.C., Newton, R.J., Dila, D.K., McLellan, S.L., 2015. Urban microbial ecology of a
685 freshwater estuary of Lake Michigan. *Elementa: Science of the Anthropocene* 3,
686 000064. <https://doi.org/10.12952/journal.elementa.000064>

687 Fisher, S.G., Gray, L.J., Grimm, N.B., Busch, D.E., 1982. Temporal succession in a desert
688 stream ecosystem following flash flooding. *Ecological Monographs* 52, 93–110.

689 Fortunato, C.S., Crump, B.C., 2011. Bacterioplankton Community Variation Across River to
690 Ocean Environmental Gradients. *Microbial Ecology* 62, 374–382.
691 <https://doi.org/10.1007/s00248-011-9805-z>

692 Fouilland, E., Trottet, A., Bancon-Montigny, C., Bouvy, M., Le Floc'h, E., Gonzalez, J.L.,
693 Hatey, E., Mas, S., Mostajir, B., Nougier, J., Pecqueur, D., Rochelle-Newall, E.,
694 Rodier, C., Roques, C., Salles, C., Tournoud, M.G., Vidussi, F., 2012. Impact of a
695 river flash flood on microbial carbon and nitrogen production in a Mediterranean
696 Lagoon (Thau Lagoon, France). *Estuarine, Coastal and Shelf Science* 113, 192–204.
697 <https://doi.org/10.1016/j.ecss.2012.08.004>

698 Gasith, A., Resh, V.H., 1999. Streams in Mediterranean Climate Regions: Abiotic Influences
699 and Biotic Responses to Predictable Seasonal Events. *Annual Review of Ecology
700 and Systematics* 30, 51–81. <https://doi.org/10.1146/annurev.ecolsys.30.1.51>

701 Ghiglione, J.F., Palacios, C., Marty, J.C., Mevel, G., Labrune, C., Conan, P., Pujo-Pay, M.,
702 Garcia, N., Goutx, M., 2008. Role of environmental factors for the vertical distribution
703 (0–1000 m) of marine bacterial communities in the NW Mediterranean Sea.
704 *Biogeosciences* 5, 1751–1764.

705 Giri, S., Qiu, Z., 2016. Understanding the relationship of land uses and water quality in
706 Twenty First Century: A review. *Journal of Environmental Management* 173, 41–48.
707 <https://doi.org/10.1016/j.jenvman.2016.02.029>

708 Jacquioud, S., Brejnrod, A., Morberg, S.M., Abu Al-Soud, W., Sørensen, S.J., Riber, L., 2017.
709 Deciphering conjugative plasmid permissiveness in wastewater microbiomes.
710 *Molecular Ecology* 26, 3556–3571. <https://doi.org/10.1111/mec.14138>

711 Jørgensen, P.S., Aktipis, A., Brown, Z., Carrière, Y., Downes, S., Dunn, R.R., Epstein, G.,
712 Frisvold, G.B., Hawthorne, D., Gröhn, Y.T., Gujar, G.T., Jasovský, D., Klein, E.Y.,
713 Klein,
714 F., Lhermie, G., Mota-Sanchez, D., Omoto, C., Schlüter, M., Scott, H.M., Wernli, D.,
715 Carroll, S.P., 2018. Antibiotic and pesticide susceptibility and the Anthropocene
716 operating space. *Nature Sustainability* 1, 632–641. <https://doi.org/10.1038/s41893->

717 018-0164-3

718 Jumas-Bilak, E., Marchandin, H., 2014. The Phylum Synergistetes, in: Rosenberg, E.,
719 DeLong, E.F., Lory, S., Stackebrandt, E., Thompson, F. (Eds.), *The Prokaryotes*.
720 Springer Berlin Heidelberg, Berlin, Heidelberg, pp. 931–954.
721 https://doi.org/10.1007/978-3-642-38954-2_384

722 Kan, J., 2018. Storm Events Restructured Bacterial Community and Their Biogeochemical
723 Potentials. *Journal of Geophysical Research: Biogeosciences* 123, 2257–2269.
724 <https://doi.org/10.1029/2017JG004289>

725 Lambert, A.-S., Morin, S., Artigas, J., Volat, B., Coquery, M., Neyra, M., Pesce, S., 2012.
726 Structural and functional recovery of microbial biofilms after a decrease in copper
727 exposure: Influence of the presence of pristine communities. *Aquatic Toxicology* 109,
728 118–126. <https://doi.org/10.1016/j.aquatox.2011.12.006>

729 Langfelder, P., Horvath, S., 2007. Eigengene networks for studying the relationships
730 between co-expression modules. *BMC Systems Biology* 1, 54.
731 <https://doi.org/10.1186/1752-0509-1-54>

732 Legendre, P., Gallagher, E.D., 2001. Ecologically meaningful transformations for ordination
733 of species data. *Oecologia* 129, 271–280. <https://doi.org/10.1007/s004420100716>

734 Llopart-Mascaró, A., Farreny, R., Gabarrell, X., Rieradevall, J., Gil, A., Martínez, M., Puertas,
735 J., Suárez, J., Río, H. del, Paraira, M., 2014. Storm tank against combined sewer
736 overflow: Operation strategies to minimise discharges impact to receiving waters.
737 *Urban Water Journal* 12, 219–228. <https://doi.org/10.1080/1573062X.2013.868499>

738 Madoux-Humery, A.S., Dorner, S., Sauvé, S., Aboufadi, K., Galarneau, M., Servais, P.,
739 Prévost, M., 2013. Temporal variability of combined sewer overflow contaminants:
740 Evaluation of wastewater micropollutants as tracers of fecal contamination. *Water*
741 *Research* 47, 4370–4382. <https://doi.org/10.1016/j.watres.2013.04.030>

742 Mahajan, M., 2019. Evolution of cellular complexity and other remarkable features in
743 Gemmataceae Complex bacterial lineages defy prokaryotic trends. (PhD Thesis).

744 Uppsala University, Disciplinary Domain of Science and Technology, Biology,
745 Department of Cell and Molecular Biology, Molecular Evolution.

746 Marti, R., Bécouze-Lareure, C., Ribun, S., Marjolet, L., Bernardin Souibgui, C., Aubin, J.-B.,
747 Lipeme Kouyi, G., Wiest, L., Blaha, D., Cournoyer, B., 2017a. Bacteriome genetic
748 structures of urban deposits are indicative of their origin and impacted by chemical
749 pollutants. *Scientific Reports* 7:13219. <https://doi.org/10.1038/s41598-017-13594-8>

750 Marti, R., Ribun, S., Aubin, J.-B., Colinon, C., Petit, S., Marjolet, L., Gourmelon, M., Schmitt,
751 L., Breil, P., Cottet, M., Cournoyer, B., 2017b. Human-Driven Microbiological
752 Contamination of Benthic and Hyporheic Sediments of an Intermittent Peri-Urban
753 River Assessed from MST and 16S rRNA Genetic Structure Analyses. *Frontiers in*
754 *Microbiology* 8:19. <https://doi.org/10.3389/fmicb.2017.00019>

755 Masters, N.M., Wiegand, A., Thompson, J.M., Vollmerhausen, T.L., Hatje, E., Katouli, M.,
756 2016. Assessing the population dynamics of *Escherichia coli* in a metropolitan river
757 after an extreme flood event. *Journal of Water and Health* 15, 196–208.
758 <https://doi.org/10.2166/wh.2016.285>

759 McLellan, S., Fisher, J., Newton, R., 2015. The microbiome of urban waters. *International*
760 *Microbiology* 141–149. <https://doi.org/10.2436/20.1501.01.244>

761 McLellan, S.L., Eren, A.M., 2014. Discovering new indicators of fecal pollution. *Trends in*
762 *Microbiology* 22, 697–706. <https://doi.org/10.1016/j.tim.2014.08.002>

763 McLellan, S.L., Huse, S.M., Mueller-Spitz, S.R., Andreishcheva, E.N., Sogin, M.L., 2010.
764 Diversity and population structure of sewage-derived microorganisms in wastewater
765 treatment plant influent. *Environmental Microbiology* 12, 378–392.
766 <https://doi.org/10.1111/j.1462-2920.2009.02075.x>

767 McLellan, S.L., Roguet, A., 2019. The unexpected habitat in sewer pipes for the propagation
768 of microbial communities and their imprint on urban waters. *Current Opinion in*
769 *Biotechnology* 57, 34–41. <https://doi.org/10.1016/j.copbio.2018.12.010>

770 McMurdie, P.J., Holmes, S., 2013. Phyloseq: An R Package for Reproducible Interactive
771 Analysis and Graphics of Microbiome Census Data. PLoS ONE 8.
772 <https://doi.org/10.1371/journal.pone.0061217>

773 Millar, J.A., Raghavan, R., 2017. Accumulation and expression of multiple antibiotic
774 resistance genes in *Arcobacter cryaerophilus* that thrives in sewage. PeerJ 5, e3269.
775 <https://doi.org/10.7717/peerj.3269>

776 Muylaert, K., Vyverman, W., 2006. Impact of a flood event on the planktonic food web of the
777 Schelde estuary (Belgium) in spring 1998. Hydrobiologia 559, 385–394.
778 <https://doi.org/10.1007/s10750-005-1081-9>

779 Newman, M.E.J., 2006. Finding community structure in networks using the eigenvectors of
780 matrices. Physical Review E 74, 036104.
781 <https://doi.org/10.1103/PhysRevE.74.036104>

782 Newton, R.J., Bootsma, M.J., Morrison, H.G., Sogin, M.L., McLellan, S.L., 2013. A Microbial
783 Signature Approach to Identify Fecal Pollution in the Waters Off an Urbanized Coast
784 of Lake Michigan. Microbial Ecology 65, 1011–1023. [https://doi.org/10.1007/s00248-](https://doi.org/10.1007/s00248-013-0200-9)
785 [013-0200-9](https://doi.org/10.1007/s00248-013-0200-9)

786 Nouha, K., Kumar, R.S., Tyagi, R.D., 2016. Heavy metals removal from wastewater using
787 extracellular polymeric substances produced by *Cloacibacterium normanense* in
788 wastewater sludge supplemented with crude glycerol and study of extracellular
789 polymeric substances extraction by different methods. Bioresource Technology 212,
790 120–129. <https://doi.org/10.1016/j.biortech.2016.04.021>

791 O'brien, R.M., 2007. A Caution Regarding Rules of Thumb for Variance Inflation Factors.
792 Quality & Quantity 41, 673–690. <https://doi.org/10.1007/s11135-006-9018-6>

793 Oksanen, J., Blanchet, F.G., Friendly, M., Kindt, R., Legendre, P., McGlinn, D., Minchin,
794 P.R., O'Hara, R.B., Simpson, G.L., Solymos, P., Henry, M., Stevens, H., Szoecs, E.,
795 Wagner, H., 2018. Vegan: Community Ecology Package. R package version 2.5-3.
796 <https://CRAN.R-project.org/package=vegan>

797 Osorio, V., Marcé, R., Pérez, S., Ginebreda, A., Cortina, J.L., Barceló, D., 2012. Occurrence
798 and modeling of pharmaceuticals on a sewage-impacted Mediterranean river and
799 their dynamics under different hydrological conditions. *Science of the Total*
800 *Environment* 440, 3–13. <https://doi.org/10.1016/j.scitotenv.2012.08.040>

801 Oursel, B., Garnier, C., Zebracki, M., Durrieu, G., Paireud, I., Omanović, D., Cossa, D.,
802 Lucas, Y., 2014. Flood inputs in a mediterranean coastal zone impacted by a large
803 urban area: Dynamic and fate of trace metals. *Marine Chemistry* 167, 44–56.
804 <https://doi.org/10.1016/j.marchem.2014.08.005>

805 Pailler, J.-Y., Guignard, C., Meyer, B., Iffly, J.-F., Pfister, L., Hoffmann, L., Krein, A., 2009.
806 Behaviour and Fluxes of Dissolved Antibiotics, Analgesics and Hormones During
807 Flood Events in a Small Heterogeneous Catchment in the Grand Duchy of
808 Luxembourg. *Water, Air, and Soil Pollution* 203, 79–98.
809 <https://doi.org/10.1007/s11270-009-9993-z>

810 Palacios, C., Zettler, E., Amils, R., Amaral-Zettler, L., 2008. Contrasting Microbial Community
811 Assembly Hypotheses: A Reconciling Tale from the Río Tinto. *PLoS ONE* 3, e3853.
812 <https://doi.org/10.1371/journal.pone.0003853>

813 Pesce, S., Fajon, C., Bardot, C., Bonnemoy, F., Portelli, C., Bohatier, J., 2008. Longitudinal
814 changes in microbial planktonic communities of a French river in relation to pesticide
815 and nutrient inputs. *Aquatic Toxicology* 86, 352–360.
816 <https://doi.org/10.1016/j.aquatox.2007.11.016>

817 Pesce, S., Lissalde, S., Lavieille, D., Margoum, C., Mazzella, N., Roubéix, V., Montuelle, B.,
818 2010a. Evaluation of single and joint toxic effects of diuron and its main metabolites
819 on natural phototrophic biofilms using a pollution-induced community tolerance
820 (PICT) approach. *Aquatic Toxicology* 99, 492–499.
821 <https://doi.org/10.1016/j.aquatox.2010.06.006>

822 Pesce, S., Margoum, C., Montuelle, B., 2010b. In situ relationships between spatio-temporal
823 variations in diuron concentrations and phototrophic biofilm tolerance in a

824 contaminated river. *Water Research* 44, 1941–1949.
825 <https://doi.org/10.1016/j.watres.2009.11.053>

826 Phillips, P., Chalmers, A., 2009. Wastewater effluent, combined sewer overflows, and other
827 sources of organic compounds to Lake Champlain. *Journal of the American Water*
828 *Resources Association* 45, 45–57. <https://doi.org/10.1111/j.1752-1688.2008.00288.x>

829 R Core Team, 2018. R: A language and environment for statistical computing. R Foundation
830 for Statistical Computing, Vienna.

831 Ramette, A., 2007. Multivariate analyses in microbial ecology: Multivariate analyses in
832 microbial ecology. *FEMS Microbiology Ecology* 62, 142–160.
833 <https://doi.org/10.1111/j.1574-6941.2007.00375.x>

834 Reoyo-Prats, B., 2014. Variations spatio-temporelles de la qualité des eaux des
835 écosystèmes fluviaux méditerranéens et premières conséquences sur la diversité
836 microbienne (Master). Université de Perpignan, France.

837 Reoyo-Prats, B., Aubert, D., Menniti, C., Ludwig, W., Sola, J., Pujo-Pay, M., Conan, P.,
838 Verneau, O., Palacios, C., 2017. Multicontamination phenomena occur more often
839 than expected in Mediterranean coastal watercourses: Study case of the Têt River
840 (France). *Science of The Total Environment* 579, 10–21.
841 <https://doi.org/10.1016/j.scitotenv.2016.11.019>

842 Reoyo-Prats, B., Aubert, D., Sellier, A., Roig, B., Palacios, C., 2018. Dynamics and sources
843 of pharmaceutically active compounds in a coastal Mediterranean river during heavy
844 rains. *Environmental Science and Pollution Research* 25, 6107–6121.
845 <https://doi.org/10.1007/s11356-017-0880-7>

846 Rout, S.P., Salah, Z.B., Charles, C.J., Humphreys, P.N., 2017. Whole-Genome Sequence of
847 the Anaerobic Isosaccharinic Acid Degrading Isolate, *Macellibacteroides fermentans*
848 Strain HH-ZS. *Genome Biology and Evolution* 9, 2140–2144.
849 <https://doi.org/10.1093/gbe/evx151>

850 Sabater, S., Elosegı, A., Ludwig, R., 2019. Summary, Implications and Recommendations for
851 the Occurrence and Effects of Multiple Stressors in River Ecosystems, in: *Multiple*

852 Stressors in River Ecosystems. Elsevier, pp. 375–380. <https://doi.org/10.1016/B978->
853 0-12-811713-2.00021-2

854 Savio, D., Sinclair, L., Ijaz, U.Z., Parajka, J., Reischer, G.H., Stadler, P., Blaschke, A.P.,
855 Blöschl, G., Mach, R.L., Kirschner, A.K.T., Farnleitner, A.H., Eiler, A., 2015. Bacterial
856 diversity along a 2600km river continuum. *Environmental Microbiology* 17, 4994–
857 5007. <https://doi.org/10.1111/1462-2920.12886>

858 SCENIHR (Scientific Committee on Emerging and Newly Identified Health Risks),
859 Assessment of the Antibiotic Resistance Effects of Biocides, 19 January 2009.
860 https://ec.europa.eu/health/scientific_committees/opinions_layman/en/biocides-
861 antibiotic-resistance/l-3/7-explanation-resistance-biofilms.htm (accessed 2020.04.05)

862 Shannon, P., Markiel, A., Ozier, O., Baliga, N.S., Wang, J.T., Ramage, D., Amin, N.,
863 Schwikowski, B., Ideker, T., 2003. Cytoscape: A Software Environment for Integrated
864 Models of Biomolecular Interaction Networks. *Genome Research* 13, 2498–2504.
865 <https://doi.org/10.1101/gr.1239303>

866 Silva, T.M., Stets, M.I., Mazzetto, A.M., Andrade, F.D., Pileggi, S.A.V., Fávero, P.R., Cantú,
867 M.D., Carrilho, E., Carneiro, P.I.B., Pileggi, M., 2007. Degradation of 2,4-D herbicide
868 by microorganisms isolated from Brazilian contaminated soil. *Brazilian Journal of*
869 *Microbiology* 38, 522–525. <https://doi.org/10.1590/S1517-83822007000300026>

870 Singh, B.K., Walker, A., 2006. Microbial degradation of organophosphorus compounds.
871 *FEMS Microbiology Reviews* 30, 428–471. <https://doi.org/10.1111/j.1574->
872 6976.2006.00018.x

873 Staley, C., Gould, T.J., Wang, P., Phillips, J., Cotner, J.B., Sadowsky, M.J., 2014. Bacterial
874 community structure is indicative of chemical inputs in the Upper Mississippi River.
875 *Frontiers in Microbiology* 5, 1–13. <https://doi.org/10.3389/fmicb.2014.00524>

876 Stewart, F.J., 2013. Where the genes flow. *Nature Geoscience* 6, 688–690.
877 <https://doi.org/10.1038/ngeo1939>

878 Taghavi, L., Merlina, G., Probst, J.-L., 2011. The role of storm flows in concentration of
879 pesticides associated with particulate and dissolved fractions as a threat to aquatic

880 ecosystems - Case study: the agricultural watershed of Save river (Southwest of
881 France). *Knowledge and Management of Aquatic Ecosystems* 06p0-06p11.
882 <https://doi.org/10.1051/kmae/2011002>

883 ter Braak, C.J.F., 1987. Unimodal models to relate species to environment. *Agricultural*
884 *University*.

885 Turner, A., Millward, G.E., 2002. Suspended Particles: Their Role in Estuarine
886 Biogeochemical Cycles. *Estuarine, Coastal and Shelf Science* 55, 857–883.
887 <https://doi.org/10.1006/ecss.2002.1033>

888 Ulrich, N., Rosenberger, A., Brislawn, C., Wright, J., Kessler, C., Toole, D., Solomon, C.,
889 Strutt, S., McClure, E., Lamendella, R., 2016. Restructuring of the aquatic bacterial
890 community by hydric dynamics associated with Superstorm Sandy. *Applied and*
891 *Environmental Microbiology* 82, 3525–3536. <https://doi.org/10.1128/AEM.00520-16>

892 U.S. Environmental Protection Agency, 2016. Clean Watersheds Needs Survey 2012. United
893 States Environmental Protection Agency 53, 1689–1699.
894 <https://doi.org/10.1017/CBO9781107415324.004>

895 Weyrauch, P., Matzinger, A., Pawlowsky-Reusing, E., Plume, S., von Seggern, D.,
896 Heinzmann, B., Schroeder, K., Rouault, P., 2010. Contribution of combined sewer
897 overflows to trace contaminant loads in urban streams. *Water Research* 44, 4451–
898 4462. <https://doi.org/10.1016/j.watres.2010.06.011>

899 Widenfalk, A., Bertilsson, S., Sundh, I., Goedkoop, W., 2008. Effects of pesticides on
900 community composition and activity of sediment microbes - responses at various
901 levels of microbial community organization. *Environmental Pollution* 152, 576–584.
902 <https://doi.org/10.1016/j.envpol.2007.07.003>

903 Wolfe, C.J., Kohane, I.S., Butte, A.J., 2005. Systematic survey reveals general applicability
904 of “guilt-by-association” within gen coexpression networks. *BMC Bioinformatics* 6,
905 227. <https://doi.org/10.1186/1471-2105-6-227>

906 Wu, C.H., Sercu, B., van de Werfhorst, L.C., Wong, J., deSantis, T.Z., Brodie, E.L., Hazen,
907 T.C., Holden, P.A., Andersen, G.L., 2010. Characterization of coastal urban

908 watershed bacterial communities leads to alternative community-based indicators.
909 PLoS ONE 5. <https://doi.org/10.1371/journal.pone.0011285>
910 Zeglin, L.H., 2015. Stream microbial diversity in response to environmental changes: review
911 and synthesis of existing research. *Frontiers in Microbiology* 6:454.
912 <https://doi.org/10.3389/fmicb.2015.00454>
913 Zhou, J., Deng, Y., Luo, F., He, Z., Yang, Y., 2011. Phylogenetic Molecular Ecological
914 Network of Soil Microbial Communities in Response to Elevated CO₂. *mBio* 2(4),
915 e00122-11. <https://doi.org/10.1128/mBio.00122-11>
916

917 **Table caption**

918 **Table 1** Summary of constrained multivariate statistical analyses. (a) Permanova
919 significance of the five models tested and the percentage of biological variance that is
920 explained by each model. (b) Axes and modelled variables significance after permanova
921 analyses from significant models in (a). p-values significance codes:
922 (**<0.001<0.01<0.05).

923

924 **Figure captions**

925 **Fig. 1** Environmental parameter dynamics in the Têt River. Seven representative dynamics
926 of environmental parameters along the flood. Samples were named as follows: tX, where X is
927 the number of hours after starting sampling time at t0, for the flood; and, on the left, SD and
928 WD for summer and winter drought samples, respectively. Dyn1 corresponds to parameters
929 with a dynamic similar to particulate organic carbon (/20 mg/l), Dyn2 to AMPA ($\mu\text{g/l}$), Dyn3 to
930 Pb (/150 $\mu\text{g/g}$), Dyn4 to pH (/70). Three parameters, Diuron, 2.4D and NO_3^- , had a unique
931 dynamic (Supplementary A2 for details, modified from Reoyo-Prats et al., 2017).

932

933 **Fig. 2** Composition and structure of microbial communities averaged across replicates. (a)
934 Principal Coordinate Analyses (PCoA) and (b) hierarchical clustering with Ward D2 linkage
935 method using Weighted-Unifrac dissimilarity computed on OTU average abundances.
936 Coloured lines indicate ANOSIM significant groups ($R=0.78$, $p<0.001$). (c) Histogram of
937 relative abundances of seven major phyla and (d) heatmap based on PCoA. For (c) and (d)
938 samples are organised according to sampling time: from summer drought (SD) to autumn
939 flood samples (tX where X is the number of hours after t0) and concluding with the winter
940 drought (WD) sample. The dotted profile is the flow level of the flood (see Fig. 1).

941

942

943

944

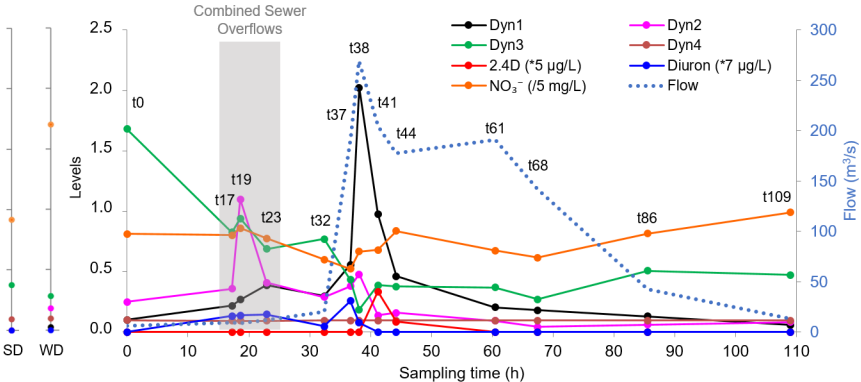
945 **Fig. 3** Redundancy analysis (RDA) biplot with scaling by species on normalised matrix of
946 OTUs with an abundance higher than 0.005%. The model explained 66.2% of the variance
947 under constraints ($p < 0.001$). Environmental variables dynamics retained are plotted in Fig. 1.
948 Significance for axes and environmental dynamics after permanova analyses are indicated,
949 p-values significance codes: *** < 0.001 ** < 0.01 * < 0.05 . For sample and environmental
950 parameter names, see Fig. 1.

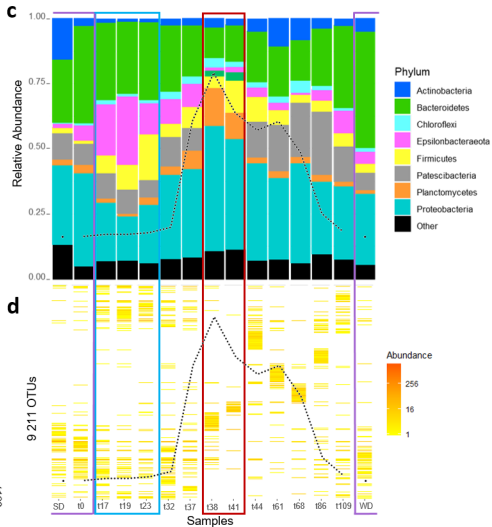
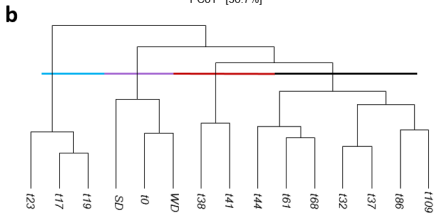
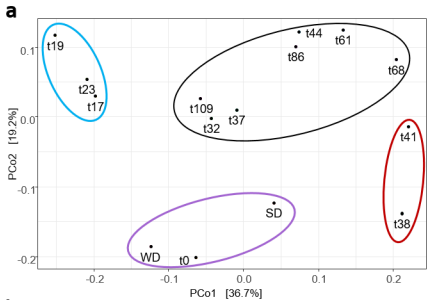
951

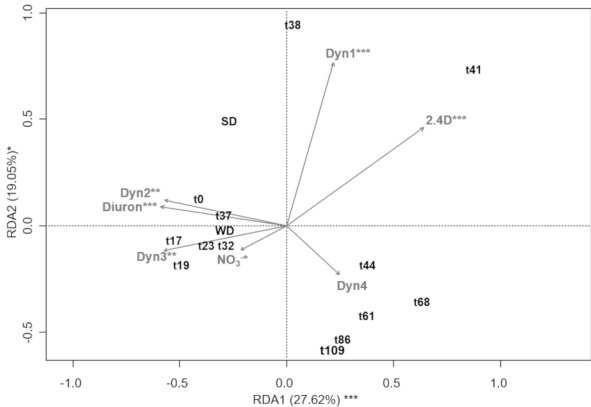
952 **Fig. 4** Module eigengene analysis. Eigengene network of thirteen modules (ModX, where
953 X=module number) significantly positively correlated to environmental dynamics from Fig. 1.
954 Each environmental dynamics is followed by module eigengene correlation value and the p-
955 value significance code as follows: *** < 0.001 ** < 0.01 * < 0.05 . OTUs are represented by
956 coloured fill according to phylum. Ellipse or round rectangle shape, respectively, represents
957 significantly and non-significantly correlated OTU abundance profiles to module eigengene.
958 The connectivity between OTUs is indicated by lines and their length is arbitrary.

959

960 **Fig. 5** Illustration of the impact of combined sewer overflows and floods on particle-attached
961 riverine bacterial communities in coastal Mediterranean rivers. Network modules contain only
962 significantly correlated OTUs to environmental dynamics represented as black rectangles
963 (see Fig. 4 for details). For each dynamic, all retrieved parameters are listed. Treemaps
964 display phyla linked to relevant taxa and their relative abundance within each module or
965 group of modules.







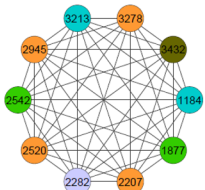
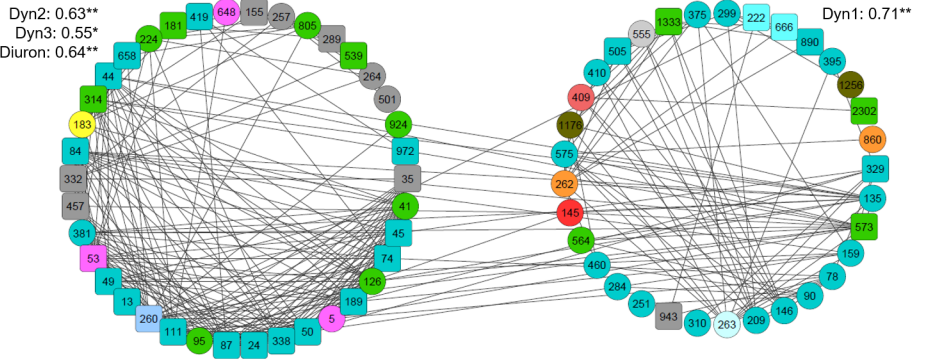
Mod1

Dyn2: 0.63**
 Dyn3: 0.55*
 Diuron: 0.64**

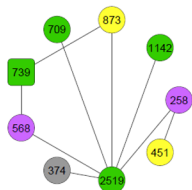
Mod2

Dyn1: 0.71**

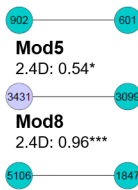
- Non-significant OTU
- Significant OTU
- Acidobacteria
- Armatimonadetes
- Bacteroidetes
- Chloroflexi
- Cyanobacteria
- Epsilonbacteraeota
- Firmicutes
- Fusobacteria
- Gemmatimonadetes
- Nitrospirae
- Patescibacteria
- Planctomycetes
- Proteobacteria
- Synergistetes
- WPS-2

**Mod3**

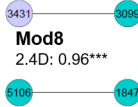
2.4D: 0.97***

**Mod4**

Dyn2: 0.66**
 Diuron: 0.9***

**Mod5**

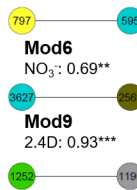
2.4D: 0.54*

**Mod8**

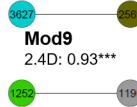
2.4D: 0.96***

**Mod11**

2.4D: 0.78***

**Mod6**

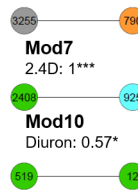
NO₃⁻: 0.69**

**Mod9**

2.4D: 0.93***

**Mod12**

Dyn2: 0.53*

**Mod7**

2.4D: 1***

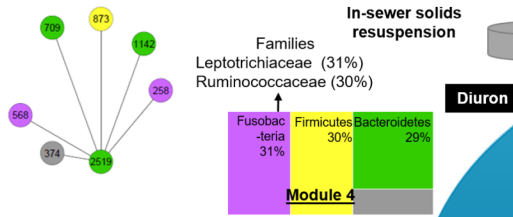
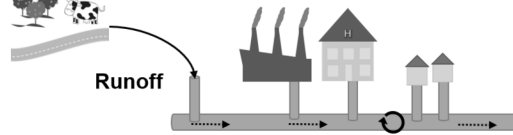
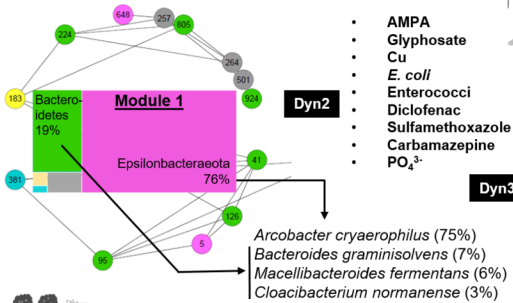
**Mod10**

Diuron: 0.57*

**Mod13**

NO₃⁻: 0.55*

Combined Sewer Overflows



Flow Peak

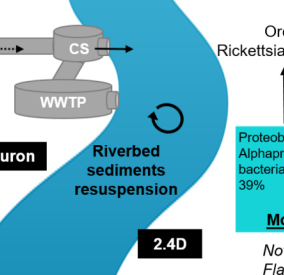
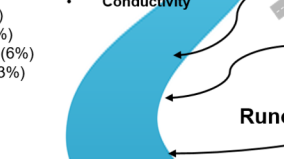
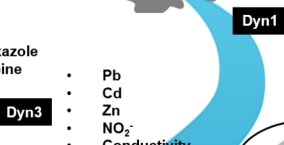
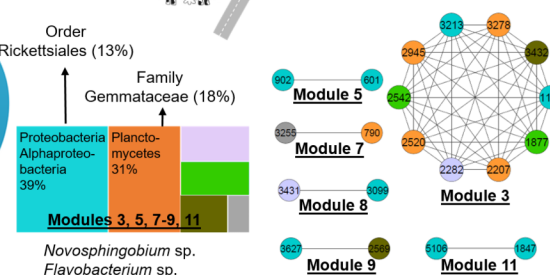
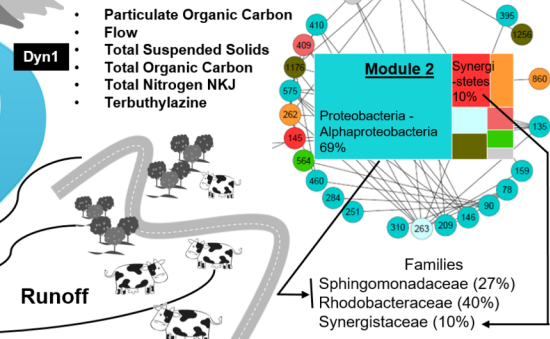


Table 1 Summary of constrained multivariate statistical analyses.

(a) Permanova significance of the five models tested and the percentage of biological variance that is explained by each model.

(b) Axes and modelled variables significance after permanova analyses from significant models in (a).

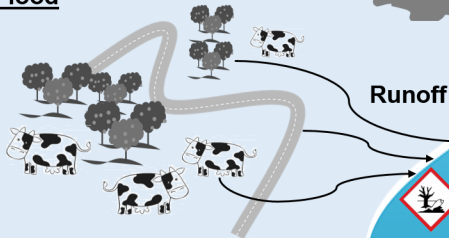
p-values significance codes: (***) < 0.001 < ** < 0.01 < * < 0.05).

a	OTUs matrice transformation	Model significance	Variance (%)
dbRDA	Jaccard	0.0120*	55.19
	Unifrac	0.003**	58.92
	Bray-Curtis	0.007**	59.70
	Morisita	0.001***	72.84
	Weighted Unifrac	0.001***	76.72
CCA		0.212	
RDA	Hellinger	0.018*	58.66

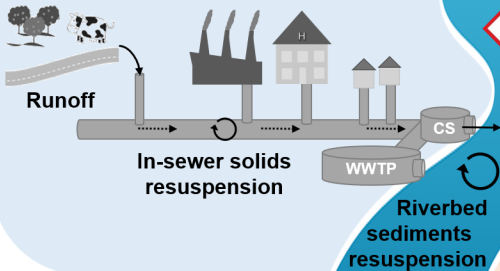
b	OTUs matrice transformation	Axes significance and variance explained (%)		Modelled variables significance						
		CAP1	CAP2	Dyn1	Dyn2	Dyn3	Dyn4	2.4D	Diuron	NO ₃ ⁻
dbRDA	Jaccard	0.006** (25.98)	0.203 (16.53)	0.090	0.065	0.050	0.428	0.002**	0.011*	0.284
	Unifrac	0.004** (30.62)	0.107 (17.89)	0.056	0.034*	0.035*	0.204	0.001***	0.010*	0.146
	Bray-Curtis	0.001** (28.85)	0.147 (17.65)	0.013*	0.012*	0.034*	0.269	0.001***	0.004**	0.142
	Morisita	0.001** (39.65)	0.031* (24.10)	0.001***	0.001***	0.003**	0.085	0.001***	0.001***	0.011***
	Weighted Unifrac	0.001** (43.04)	0.003* (21.87)	0.001***	0.001***	0.003**	0.104	0.002**	0.002**	0.001***
		Axes significance and variance explained (%)		Modelled variables significance						
		RDA1	RDA2	Dyn1	Dyn2	Dyn3	Dyn4	2.4D	Diuron	NO ₃ ⁻
RDA	Hellinger	0.008** (29.12)	0.160 (17.99)	0.034*	0.068	0.080	0.441	0.002**	0.007**	0.179

Storm Event

- Flood**



- Combined Sewer Overflows**



Water Samples



**Pollutant-resistant
and Pathogenic
Taxa**

**Risk on Human and
Ecosystem Health**

**Key
Players**

Potential **biosignatures** of
combined stressors